
Abstract

The increasing share of renewable energy sources (RES) combined with their dependence on weather poses a critical challenge for energy systems. This study investigates the impact of targeting a balanced distribution of wind and photovoltaic (PV) capacity on reducing periods of low renewable generation, known as RES droughts. Three different RES models are used to estimate the capacity factors for different installed capacities of wind and PV energy. The skill of the RES models is quantified by comparing capacity factor time series to observed data and by assessing their representation of observed RES droughts. The RES models are used to generate a 45-year hourly time series of RES capacity factor, enabling analysis of the frequency, duration and return periods of RES droughts at a climatological scale. Results show the importance of using an accurate, validated RES model for RES drought risk assessment. The addition of PV capacity to a wind-dominated system results in a large reduction in the frequency and duration of RES droughts, as well as reducing extremes and seasonal drought patterns. These findings underscore the importance of diversification in RES capacity to enhance energy security and resilience.

Keywords: RES Drought, Wind Power, Solar PV Power, Renewable Energy Sources, Return Periods

1. Introduction

The EU aims to generate at least 69% of its electricity from renewable energy sources (RES) by 2030, up from 41% in 2022 [1]. While this transition is essential for reducing greenhouse gas emissions, it also highlights the challenge of managing the variability of weather-dependent energy sources such as wind and photovoltaic (PV) power. This challenge is compounded by the increasing electrification of energy sectors, which places greater demand on the power system and makes it more sensitive to meteorological conditions [2, 3, 4]. Periods of low renewable generation, known as *Dunkelflaute* or RES droughts, pose significant risks to system adequacy and energy security, emphasizing the need for a resilient energy system to meet both growing electricity demand and decarbonization targets.

This study focuses on Ireland, a region with a strong reliance on wind power, which has ambitious targets for PV power expansion. This case study

15 provides valuable insights into the potential benefits of diversifying the re-
 16 newable energy mix on RES droughts. The performance of different RES
 17 models are compared, and a 45-year time series of RES generation is pro-
 18 duced. The results highlight the role of increased PV capacity in reducing
 19 RES drought risks, offering insights for policymakers and energy planners.

20 For this study, a RES drought event is defined as occurring when the
 21 average capacity factor (CF) remains below a fixed threshold for a given du-
 22 ration, following the methodology used in other research [5, 6, 7, 8]. Alterna-
 23 tive methods exist for defining RES droughts. One approach uses relative CF
 24 thresholds that change over the year to account for seasonal variations in re-
 25 newable energy generation [9, 10, 11, 12, 13]. Another common method relies
 26 on percentile-based thresholds, where drought events are defined by identi-
 27 fying periods of unusually low generation relative to historical production
 28 levels, typically based on the lowest production percentiles [12, 14]. Addi-
 29 tionally, some studies combine these definitions with metrics that incorporate
 30 the demand side of energy consumption, analysing the balance between sup-
 31 ply and demand during drought periods [9, 10, 12, 14]. In this paper, the
 32 focus is exclusively on energy generation, and a fixed threshold approach to
 33 define RES droughts is used, which facilitates consistent inter-comparison
 34 between scenarios with different installed wind and PV capacities.

35 RES droughts are identified using onshore wind and PV CF time series.
 36 In this study, three different datasets are used, all of which are driven by
 37 ERA5 data [15]. Two of the datasets are part of C3S Energy (C3S-E), an
 38 energy-based operational dataset produced by the EU Copernicus Climate
 39 Change Service [16, 17]. One of the n 5 offers a discussion of the results in
 40 the context of energy reliability and future planning, followed by the main
 41 conclusions and recommendations for further research.

42 2. Data

43 C3S-E datasets provides CF time series aggregated at the national scale,
 44 while the other provides the CF time series at each grid point, at the ERA5
 45 resolution of 0.25° . The third dataset was generated using the Atlite model [18],
 46 which converts the ERA5 atmospheric data to a generation time series using
 47 specified wind turbine and PV panel models. Atlite is an open-source tool
 48 developed by PyPSA [18] and is widely used for estimating wind and PV
 49 generation [7, 19, 20, 21].

The datasets used in this study are detailed in section 2, which describes their characteristics and relevance for evaluating RES droughts. Section 3 outlines the RES models used to simulate wind and PV generation and provides the methodology for defining and identifying RES drought events, including the thresholds and metrics applied. In section 4, the models are first verified against observed energy data to assess their accuracy, followed by an analysis of RES drought occurrences for two scenarios with different ratios of installed wind to PV capacities. Finally, section

This study uses publicly available datasets to construct and validate the models for estimating the CF of wind and PV energy. The primary data sources include: EirGrid and SONI, the transmission system operators (TSO) for the Republic of Ireland and Northern Ireland, respectively; the ERA5 reanalysis dataset; and the C3S-E datasets.

2.1. Wind and PV Capacity and Availability

EirGrid, the TSO for the Republic of Ireland, and SONI, the Northern Ireland TSO, provide detailed datasets on all wind and PV farms across the island of Ireland (Republic of Ireland and Northern Ireland) from 1990 to the present [22]. These datasets include information such as each farm’s installed capacity, name, and connection date. To enhance the accuracy of this data, the longitude and latitude for each farm were manually determined through online searches. For simplicity, this data will be referred to as originating from EirGrid, as all-island data was directly obtained from EirGrid, and the combined regions of the Republic of Ireland and Northern Ireland will be referred to as Ireland throughout the remainder of this document.

The spreadsheet available from the EirGrid website contains two key variables: generation and availability. Generation is the energy that a RES farm actually contributed to the grid, which may include limitations introduced by the TSO to maintain grid stability, such as constraints and curtailment. Availability represents the energy that would have been generated from a RES farm if no grid constraints had been applied, making it representative of the weather-related response. Generation and availability values are available from 2014 onward for wind power and from 2018 onward for PV power, although PV availability data only became present in the Republic of Ireland in 2023. This study focuses on availability for all analyses.

84 2.2. Atmospheric Variables

85 Atlite and C3S-E datasets are driven by the ERA5 reanalysis [15], pro-
 86 duced by the European Centre for Medium-Range Weather Forecasts (ECMWF).
 87 This global gridded dataset provides hourly atmospheric variables from 1940
 88 to the present at a horizontal resolution of 0.25° . It is widely used for esti-
 89 mating PV and wind energy [7, 16, 23, 24]. Table 1 lists the ERA5 variables
 90 used by Atlite and C3S-Energy.

Table 1: ERA5 variables used to calculate wind and PV generation

ERA5 name	variable
100 metre zonal and meridional wind speed	u_{100}, v_{100}
2 metre temperature	$t2m$
Surface net solar radiation	ssr
Surface solar radiation downwards	$ssrd$
Top of atmosphere incident radiation	$tisr$
Total sky direct solar radiation at surface	$fdir$

91 2.3. C3S Energy

92 The EU Copernicus Climate Change Service developed the C3S-E renew-
 93 able energy dataset for Europe [16], using ERA5 atmospheric variables and
 94 weather-to-energy models. This dataset provides hourly CF for wind and PV
 95 energy from 1979 to the present. The data are available on the same grid as
 96 the ERA5 data, which has a horizontal resolution of 0.25° . The time series
 97 are also available for download at two aggregated scales: regional (NUTS 2)
 98 and national.

99 The C3S-E dataset estimates wind energy using wind speeds at 100 me-
 100 tres (u_{100}, v_{100}) and a standard turbine model, the Vestas V136/3450, with
 101 a fixed hub height of 100 meters. This choice is based on expert advice and
 102 the trend in wind turbine installation. The PV generation model used by
 103 C3S-E uses two ERA5 variables: surface solar radiation downwards ($ssrd$)
 104 and air temperature ($t2m$). PV generation is calculated multiple times, us-
 105 ing the same model with different azimuth and tilt angles. The results are
 106 aggregated based on a statistical distribution of the module angles based on
 107 the geographical location [25].

108 3. Methods

109 This study uses three datasets to analyse RES droughts across the island
110 of Ireland. Data downloaded from C3S-E were used to obtain two datasets:
111 one based on national-level data (C3S-E N), and another on grid-level data
112 (C3S-E G). The third dataset was computed using the Atlite model (Atlite).

113 3.1. C3S-Energy National

114 For national-level analyses, the aggregated CF time series provided by
115 C3S-E were used at two levels: Republic of Ireland (NUTS0: IE) and North-
116 ern Ireland (NUTS2: UKN0). These are based on the assumption by C3S-E
117 that RES generation occurs at every ERA5 grid point in Ireland. We com-
118 puted a weighted average of these, based on the installed capacity of each
119 one, to represent the total CF for Ireland.

120 3.2. C3S-E Gridded

121 The gridded dataset from C3S-E was used to create CF datasets which
122 account for the location of RES farms in Ireland. A list of the RES farms in
123 Ireland was compiled, including each farm’s latitude, longitude and installed
124 capacity. Using these coordinates, the nearest grid point on the C3S-E grid
125 was identified for each farm. The CF values from the C3S-E dataset corre-
126 sponding to these grid points were retrieved. A weighted average of the CF
127 values was calculated, with the installed capacity of each farm serving as the
128 weight, to construct the CF time series for Ireland. This process resulted in
129 a time series of RES generation for each energy source (wind and PV) for
130 Ireland, which takes the location of the RES farms into account.

131 3.3. Atlite

132 Atlite transforms weather data into energy data using the gridded ERA5
133 data and the locations of existing RES farms, as described in C3S-E G.
134 ERA5 data for wind speed at 100 metres (u_{100} , v_{100}) are used to calculate
135 wind generation, while the ERA5 radiation variables (ssr , $ssrd$, $tisr$, and
136 $fdir$) and air temperature ($t2m$) are used to calculate PV generation. A
137 key distinction between C3S-E and Atlite lies in their representation of wind
138 turbines and PV panels. This study identifies the most appropriate wind
139 turbine power curve to use from the 121 power curves made available by
140 Renewables.ninja [26]. The selection of a specific wind turbine and PV panel
141 characteristics is further discussed and explained in section 4.1.

142 3.4. *Energy Scenarios*

143 In addition to analysing wind and PV generation separately, a combined
144 CF was computed for each model by averaging wind and PV generation,
145 weighted by their installed capacities at the end of 2023 (5.9 GW for wind
146 power and 0.6 GW for PV power). This configuration is referred to as the
147 91W-9PV scenario, reflecting the distribution of 91% wind and 9% PV ca-
148 pacity. Given that PV capacity in Ireland is low in 2023, and to explore how
149 a more balanced distribution of wind and PV capacities might impact RES
150 droughts, this study also considered a second scenario, referred to as 57W-
151 43PV, where the installed PV capacity is assumed to increase to 8.6 GW,
152 while wind capacity rises to 11.45 GW. These values are based on targets
153 outlined in the roadmap published by the 2024 Climate Action Plan [27].
154 This study does not include offshore wind in the analysis. Recent reports
155 suggest that even by 2030, Ireland is unlikely to have any significant new off-
156 shore wind farms, with projected offshore capacity expected to remain near
157 zero using realistic scenarios [28].

158 New time series were generated for both the Atlite and C3S-E G PV mod-
159 els, incorporating a revised distribution of installed capacity across Ireland
160 as specified in the roadmap. For wind power, the CF time series remains un-
161 changed, as significant shifts in the location of wind farms are not expected.
162 In total, twelve CF time series were analysed in this study, six for individual
163 wind and PV CF (three models for each source) in the 91W-9PV scenario,
164 and an additional six time series that include the combined CF for 91W-9PV
165 and 57W-43PV scenarios across the different models.

166 It is important to note that the specific capacity values used in this study
167 are illustrative and are not intended to reflect precise future realities. Instead,
168 they serve to explore the impact of transitioning from a wind-dominated sys-
169 tem (91W-9PV) to a more evenly distributed system (57W-43PV). This ap-
170 proach allows for a comparative analysis between the two scenarios, assessing
171 how the balance of RES capacity affects the occurrence of RES droughts.

172 3.5. *RES Drought Definition*

173 In this study, a RES drought event was defined as occurring when the
174 24-hour moving average of CF remains below a fixed threshold of 0.1 for
175 a period of longer than 24 hours. The choice of this threshold is somewhat
176 arbitrary, but aligns with similar studies on low renewable energy production
177 [5, 6, 8]. By using a 24-hour moving average, fewer but longer-lasting events
178 were captured compared to using the raw CF time series, which can be more

179 sensitive to short-term fluctuations. A fixed threshold approach was chosen
 180 in this study to enable consistent inter-comparison between datasets.

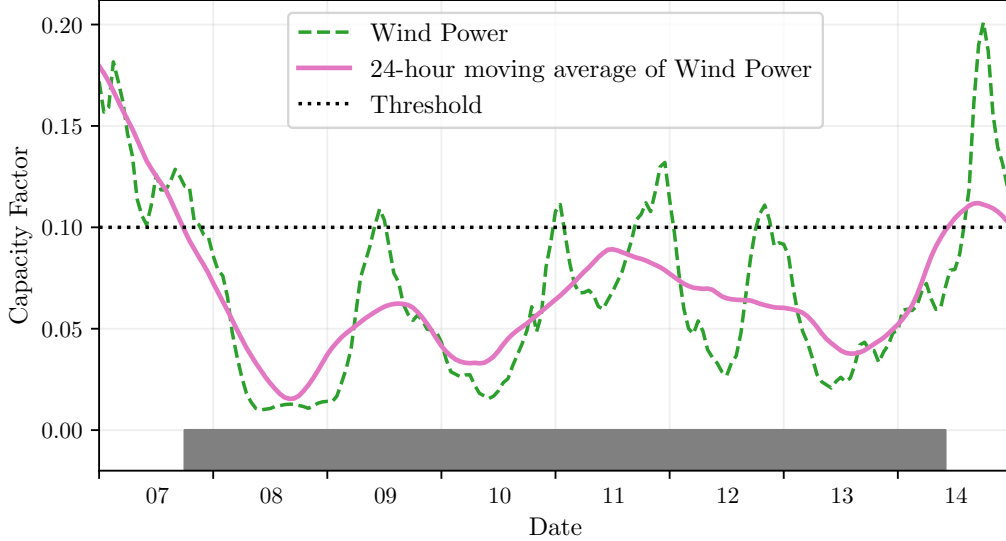


Figure 1: Wind time series of CF (green) and its 24-hour moving average (pink) from the 7th to the 15th of July 2021. The black dashed line indicates the CF threshold. The grey bar shows the period identified as a wind drought under our definition

181 The moving average approach smooths out short-term fluctuations, so
 182 that brief periods above the threshold do not interrupt an otherwise con-
 183 tinuous low-CF period (Fig. 1). This means that a single hour above the
 184 threshold does not "break" a drought event if it is surrounded by prolonged
 185 low-generation hours. As a result, fewer but longer-lasting drought events
 186 are identified, which may better reflect real-world conditions where energy
 187 supply constraints persist over extended periods.

188 4. Results

189 4.1. Verification

190 The accuracy of the datasets used in this study was verified, before con-
 191 tinuing to the analysis of RES droughts. For the verification process, time-
 192 varying values of installed capacity were used to account for changes in RES
 193 development over the verification period. This step allowed us to assess how

194 well the datasets represent the production of renewable energy by comparing
 195 them against observed data.

196 4.1.1. Wind Energy

197 The C3S-E datasets use the Vestas V136/3450 wind turbine power curve,
 198 (Fig. 2a). The Atlite model allows the user to specify the power curve.
 199 We considered the 121 power curves available for download from Renew-
 200 ables.ninja [26]. For each power curve, Renewables.ninja also provides four
 201 associated smoothed power curves. The smoothing is done using a Gaus-
 202 sian filter with different standard deviations that depend on the wind speed.
 203 A separate wind CF time series for Ireland was generated for each of the
 204 wind turbine power curves and smoothing levels. The performance of each
 205 CF time series was then assessed based on four skill scores: correlation co-
 206 efficient (CC), root mean square error (RMSE), mean bias error (MBE),
 207 and area under the curve. The area under the curve was calculated from
 208 histograms of the hourly CF values for the most recent decade, 2014-2023.
 209 Based on these metrics, the most representative power curve for Ireland was
 210 the Enercon E112.4500 power curve with the $0.3w$ smoothing filter.

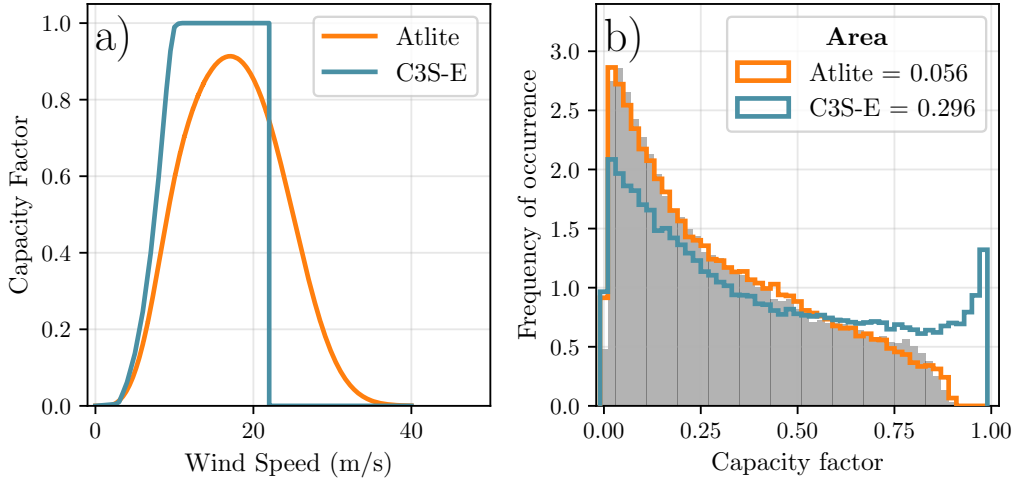


Figure 2: a) Power curves of the Enercon E112.4500 with a $0.3w$ smoothing filter used by Atlite (orange) and the Vestas V136/3450 used by C3S-E (blue) b) Histograms of wind CF for Ireland from Atlite (orange), C3S-E (blue) and Observed (shaded)

211 The smoothing of the wind turbine power curve represents losses associ-
 212 ated with each turbine, as well as losses such as wake effects between turbines,

213 which are important when modelling wind energy on larger spatial scales.
 214 The histogram in Fig. 2b shows that the C3S-E power curve tends to under-
 215 estimate low CF values and overestimate higher ones, whereas the smoothed
 216 Atlite power curve more closely follows the recorded wind availability data
 217 from EirGrid.

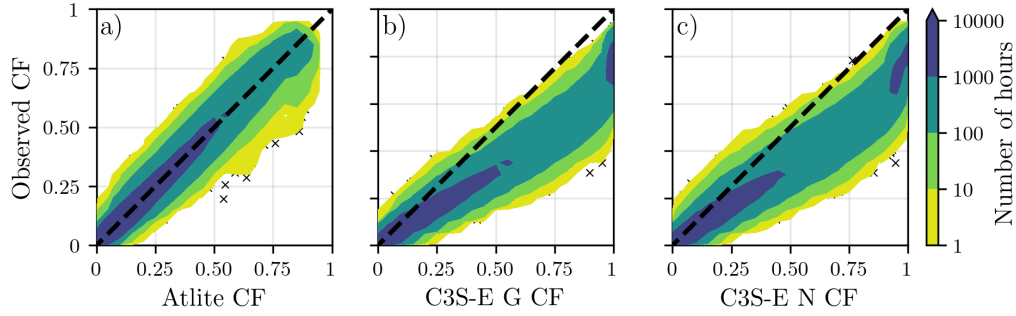


Figure 3: Wind CF density plot of the observed CF (vertical axes) and modelled (horizontal axes) CF data for the a) Atlite, b) C3S-E G and c) C3S-E N models

218 The effect of the difference between the power curves is also visible in
 219 Fig. 3, which shows a density plot of wind CF values. The two C3S-E datasets
 220 are shown to overestimate the observed CF, whereas the Atlite model is in
 221 good agreement with the observed data. The skill scores presented in Table 2
 222 show that Atlite performs better than the C3S-E datasets for all of the skill
 223 scores.

	Atlite	C3S-E G	C3S-E N
CC	0.981	0.972	0.970
RMSE	0.045	0.177	0.162
MBE	-0.003	0.137	0.121

Table 2: Skill scores for wind power for the three datasets compared to observed data

224 Fig. 4 shows the average annual number of wind drought events during
 225 the 2014 to 2023 validation period. The figure reveals that Atlite presents
 226 the best overall agreement with the observed frequency and duration of wind
 227 drought events. This pattern is particularly evident for shorter-duration
 228 events, which are the most frequent.

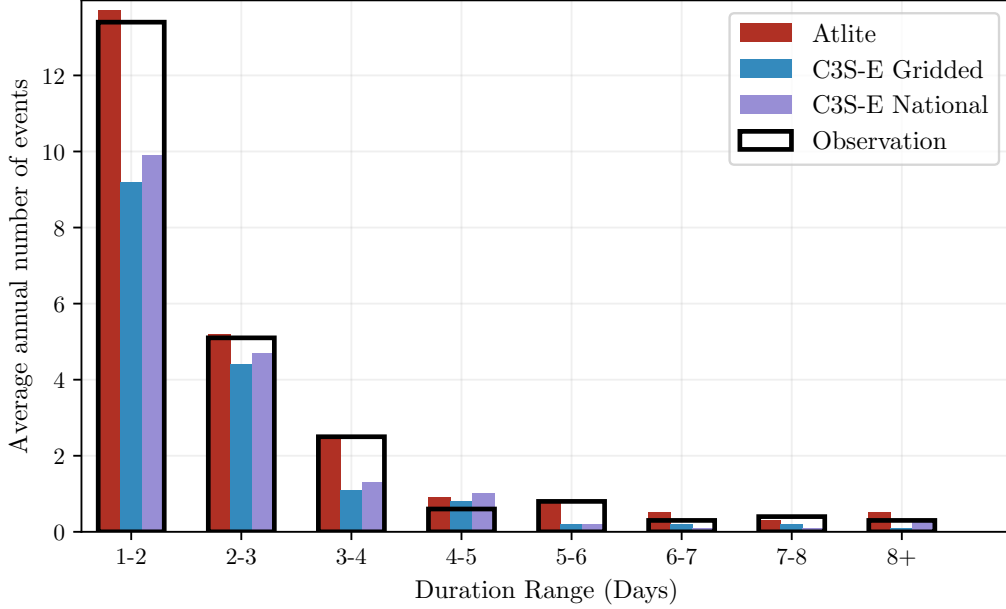


Figure 4: Average annual number of wind drought events for Atlite (red), C3S-E G (blue), C3S-E N (purple), and the observed data (black outline). The wind droughts are identified from 2014 to 2023, considering the actual capacity of the system at any given time

229 4.1.2. PV Energy

230 The Atlite model allows the user to select certain PV panel characteristics.
 231 In this study, the three PV panel types available in the Atlite model were
 232 considered (CSi, CdTe, Kaneka). Following the same methodology as in the
 233 previous section, the three available models were compared using four skill
 234 scores (CC, RMSE, MB, and area under the curve). Based on the best-
 235 performing metrics, the Breyer PV panel model was selected [29], using the
 236 Kaneka Hybrid panel option. For all PV farm locations, the azimuth angle
 237 is fixed at 180° (due south), and the optimal tilt angle option is applied.

238 The PV installed capacity available on the spreadsheets from EirGrid
 239 represents the Maximum Export Capacity (MEC) and does not accurately
 240 reflect the installed PV capacity. To enable actual PV generation potential
 241 to be modelled correctly, installed capacities were set at 1.4 times the MEC
 242 values. This scaling factor was estimated by analysing proprietary data from
 243 individual PV farms provided by EirGrid, which showed that, on average,
 244 assuming that the installed capacities of farms exceed their MEC values by

245 40% yields the best agreement with the observed availability.

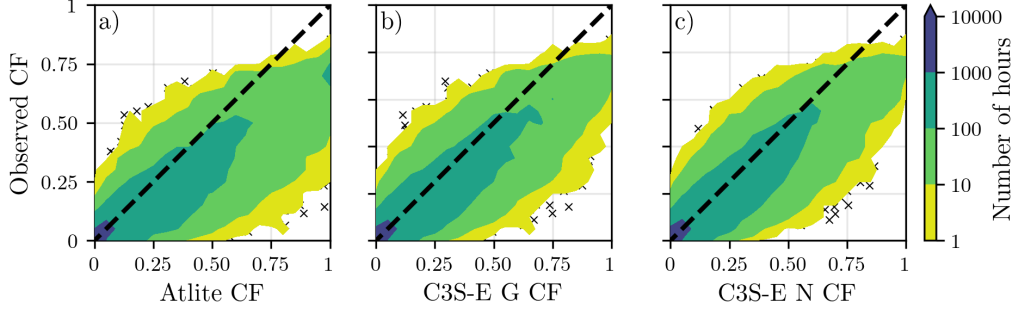


Figure 5: PV CF density plot of the observed (vertical axes) and modelled (horizontal axes) CF series for the a) Atlite, b) C3S-E G and c) C3S-E N models

246 Figure 5 shows that the three datasets have a similar tendency to overesti-
 247 mate the CF compared to the observed values, especially for high CF values.
 248 The skill scores presented in Table 3 indicate that C3S-E G performs best
 249 overall, with the lowest RMSE and a high correlation coefficient, suggesting
 250 a closer match to observed data. All models show a slight positive bias, with
 251 Atlite exhibiting a slightly lower correlation and higher RMSE.

	Atlite	C3S-E G	C3S-E N
CC	0.921	0.931	0.931
RMSE	0.119	0.090	0.113
MBE	0.046	0.027	0.021

Table 3: Skill scores for PV CF for the three datasets compared to observed data

252 Fig. 6 shows the number of PV drought events during the 2023 validation
 253 period across different duration ranges. The figure reveals partial agreement
 254 between the three datasets and the observed data, with consistent results
 255 noticed for duration ranges of 1-2, 3-4, 7-8, and 8+ days. However, dis-
 256 crepancies appear in the other ranges, where the models diverge from the
 257 observed data. The main challenge in validating PV data stems from the
 258 recent installation of a large share of Ireland’s PV capacity, leading to un-
 259 certainties in PV generation data and the actual generating capacity in the
 260 first few months after each farm is connected. With over 65% of the total
 261 PV capacity installed in 2023, these data uncertainties significantly impact
 262 the ability to perform rigorous validation for PV drought events.

263 Nevertheless, the goal of this analysis is to assess the combination of wind
 264 and PV generation, where the complementary nature of these energy sources
 265 mitigates the limitations seen in PV-only results.

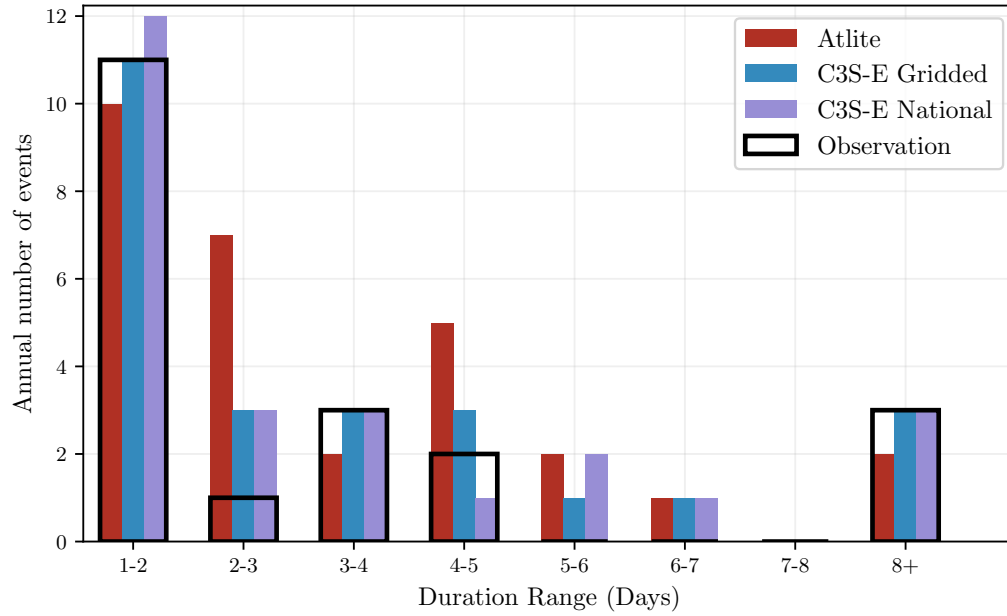


Figure 6: Number of PV drought events for Atlite (red), C3S-E G (blue), and C3S-E N (purple) and the observed data (black outline). The PV droughts are identified for 2023, considering the actual capacity of the system at any given time

266 4.2. Analysis

267 In this section, RES drought events are evaluated under two different
268 scenarios with fixed installed capacities: the 91W-9PV scenario, with 5.9 GW
269 of wind capacity and 0.6 GW of PV capacity; and the 57W-43PV scenario,
270 where wind capacity comprises 11.45 GW and PV capacity increases to 8.6
271 GW. Both scenarios were driven by 45 years of ERA5 data. Using the RES
272 drought identification process described in Section 3.5, wind and PV droughts
273 are first analysed separately before presenting the results for combined (wind
274 + PV) RES droughts under both scenarios.

275 4.2.1. Annual Number of RES Droughts

276 The first part of the analysis examines the annual number of RES drought
277 events across the three datasets. When only wind energy is considered
278 (Fig. 7a), the number of events decreases as the duration range increases,
279 with very few events lasting more than seven days. In the case of only PV
280 energy (Fig. 7b), the number of events also declines as the duration range
281 extends from one to eight days, followed by a slight increase for longer dura-
282 tions. This increase is due to extended low-generation periods occurring from
283 November to March, depending on the dataset. When comparing wind and
284 PV results (Fig. 7a & b), the median, first, and third quartiles for PV are
285 consistently higher than or equal to those for wind, across all duration ranges
286 and datasets. This is due to the typically lower CF of PV power compared
287 to wind power, especially in a region such as Ireland where solar potential
288 is limited. PV generation is also zero at night and constrained by the daily
289 solar cycle, leading to a naturally higher frequency of drought events in PV
290 compared to wind.

291 Fig. 7c & d show the combination of wind and PV under the two capacity
292 scenarios. In the 91W-9PV scenario (Fig. 7c), the identified RES droughts
293 closely match those for wind alone, which is expected due to the dominance
294 of installed wind capacity. In contrast, the 57W-43PV scenario (Fig. 7d)
295 shows a clear reduction in the number of drought events across all datasets
296 and durations, with a decrease of the total number of events of 56% for Atlite,
297 52% for C3S-E G, and 50% for C3S-E N. This reduction is attributed to the
298 anti-correlation between wind and PV generation.

299 The median, first, and third quartiles for the Atlite dataset are consis-
300 tently greater than or equal to those of the other two datasets, regardless of
301 the duration range or type of renewable energy considered. This difference
302 arises from the wind turbine power curve model used in the C3S-E datasets,

303 which tends to overestimate the wind CF (Fig. 3). As a result, the overall
 304 number of RES droughts is underestimated in the C3S-E datasets compared
 305 to Atlite.

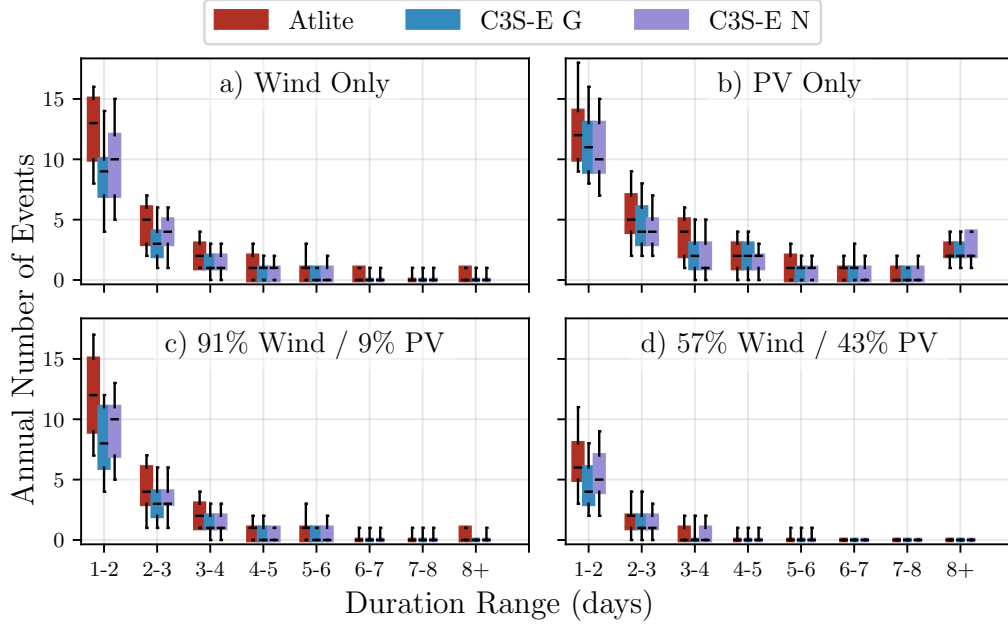


Figure 7: Annual number of RES droughts (from 1979 to 2023) for a) Wind, b) PV, and the combination for the c) 91W-9PV and d) 57W-43PV scenarios for Atlite (red), C3S-E G (blue), and C3S-E N (purple). The x-axis represents duration ranges in days (lower bound included), while the y-axis indicates the annual number of events. The boxes display the first and third quartiles and the median is marked by a black line. The whiskers indicate the 5th and 95th percentiles

306 4.2.2. *Return Periods of RES Drought Duration*

307 The RES drought events identified over the 45-year period were used to
308 calculate the return periods for different RES drought durations. A return
309 period is the estimated average time interval between events of a specified du-
310 ration or intensity (not to be confused with the frequency of their occurrence
311 within a fixed time frame). Fig. 8 illustrates the return periods for varying
312 RES drought durations, highlighting how often different drought lengths are
313 likely to occur across the datasets. This analysis provides insight into the
314 frequency and likelihood of prolonged low-generation periods, which is cru-
315 cial for evaluating the potential impact of RES droughts on energy reliability
316 and security of supply.

317 The duration of wind droughts (Fig. 8a) increases in a log-linear fash-
318 ion across the three datasets. The log-linear trend indicates a predictable
319 relationship between drought duration and occurrence, with longer wind
320 droughts becoming exponentially less likely as duration increases.

321 In the case of PV droughts (Fig. 8b), Atlite behaves differently than the
322 two C3S-E datasets. The Atlite results show a log-linear increase but reach
323 higher values in general with the longest event lasting forty days. For C3S-E
324 G and C3S-E N, the duration of PV droughts increases in a log-linear pattern
325 for events lasting less than 16 days. Beyond this duration, there is a sharp
326 rise in drought duration for events up to a one-year return period. This
327 sudden increase reflects the impact of winter on PV generation in Ireland, as
328 PV output often remains below the CF threshold for extended periods during
329 winter months. The difference between Atlite and the C3S-E results arises
330 from differences in the datasets near the threshold of 0.1 CF. Atlite remains
331 slightly above the threshold more frequently during these conditions, leading
332 to shorter, more fragmented drought events. In contrast, C3S-E G and C3S-
333 E N tend to fall below the threshold in similar conditions, resulting in longer
334 continuous drought periods, especially during winter. This sensitivity to
335 the threshold highlights how slight model differences can have substantial
336 effects on drought duration estimates, particularly for PV in low-generation
337 conditions.

338 For the 91W-9PV scenario (Fig. 8c), the return periods mirror those of
339 Fig. 8a, due to the low levels of installed PV capacity. In the 57W-43PV
340 scenario (Fig. 8d), the return periods for RES droughts increase across all
341 durations. For example, the return period for a five-day drought event (shown
342 by the vertical dashed lines in Fig. 8) extends from roughly six months for

the 91W-9PV scenario, to four years for the 57W-43PV scenario in the Atlite dataset, and from about fifteen months to around five years in the two C3S-E datasets.

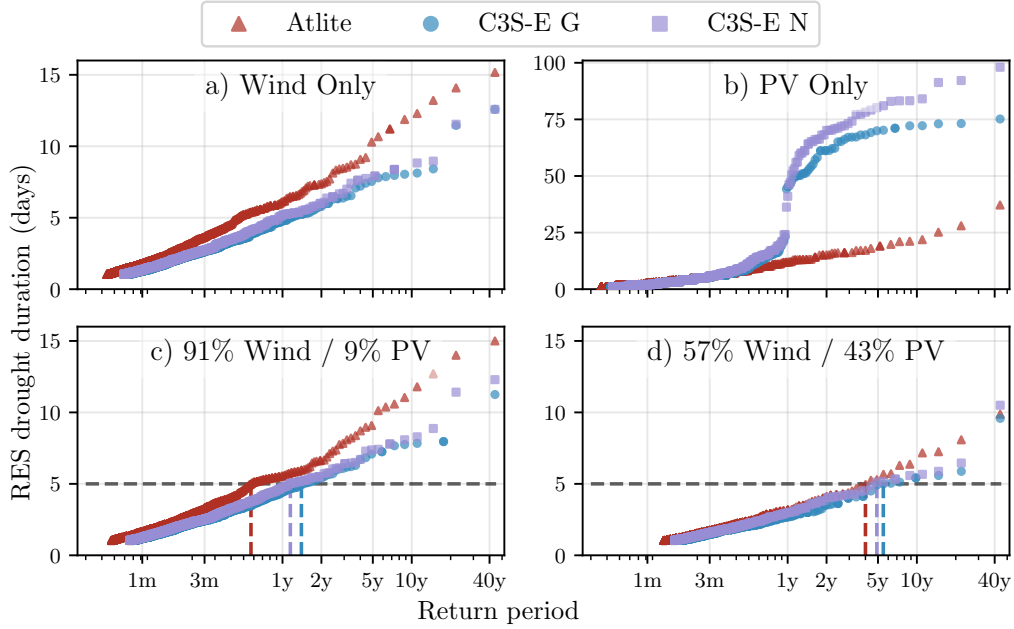


Figure 8: Return periods of the duration of RES droughts (from 1979 to 2023) for a) Wind, b) PV, and the combination for the c) 91W-9PV and d) 57W-43PV scenario, for Atlite (red triangle), C3S-E G (blue circle), and C3S-E N (purple square). The x-axis represents the return period time in a log-scale and the y-axis indicates the duration of RES drought associated with it. The horizontal dashed line marks the 5-day return period, with coloured vertical dashed marking its return period for each dataset

Across Fig. 8a, c, and, d, the return periods in the Atlite dataset are consistently higher than those in the two C3S-E datasets. For instance, in the 91W-9PV scenario (Fig. 8c), an event with a one-year return period lasts six days in the Atlite dataset, compared to only five days in the C3S-E datasets. This difference underscores the importance of model selection when quantifying RES droughts, as each model’s assumptions and parametrisations significantly influence drought duration estimates. Additionally, in all four graphs, the similarity between results from the two C3S-E datasets suggests that assumptions in the Atlite model—such as wind turbine power curve selection and PV panel specifications—have a greater impact on RES drought

356 duration estimates than the precise geographic distribution of RES farms
357 when studying the return periods of RES droughts.

358 4.2.3. Seasonal Distribution of RES Droughts

359 The seasonality of RES droughts was analysed by comparing the percent-
360 age of hours in each month classified as part of a RES drought.

361 The percentage of hours that are part of a wind drought (Fig. 9a) are
362 higher in summer than in winter. In the Atlite dataset, for instance, an aver-
363 age of 24% of hours in summer (June-July-August) are identified as wind
364 droughts, compared to only 4% in winter (December-January-February).
365 This seasonal variation is less prominent for the two C3S-E datasets com-
366 pared to the Atlite one. This difference can be linked to the shape of the two
367 power curves (Fig. 2). CFs near or under the 0.1 threshold are produced by
368 higher wind speeds for the Atlite power curve than for the C3S-E one. In
369 contrast, the results for PV droughts (Fig. 9b) show a higher percentage in
370 winter, with PV droughts occurring over 60% of the time regardless of the
371 dataset. The Atlite results show a higher percentage of PV drought hours
372 for wind, and a slightly lower percentage for PV, compared to the two C3S-E
373 datasets.

374 Similar to previous results, the 91W-9PV scenario (Fig. 9c) shows pat-
375 terns comparable to the ones for wind droughts (Fig. 9a). However, in the
376 91W/9PV scenario, the number of hours classified as RES droughts in sum-
377 mer decreases slightly compared to the wind-only scenario. This reduction
378 can be explained by the contribution of PV generation during the summer
379 months in the 91W-9PV scenario, even though it constitutes only 11% of
380 total capacity. Since the number of RES drought hours for PV in summer is
381 near zero, this small contribution has a noticeable impact on reducing over-
382 all drought hours. In the 57W-43PV scenario (Fig. 9d), all three datasets
383 show a reduction in monthly RES drought frequency. Annual reductions in
384 median RES drought frequency are observed across the datasets, dropping
385 from 14% to 5% for Atlite, from 8% to 3% for C3S-E G, and from 9% to
386 4% for C3S-E N. The balanced mix of wind and PV power in this scenario
387 reduces the seasonal signal overall and significantly decreases the percentage
388 of RES drought hours in the summer.

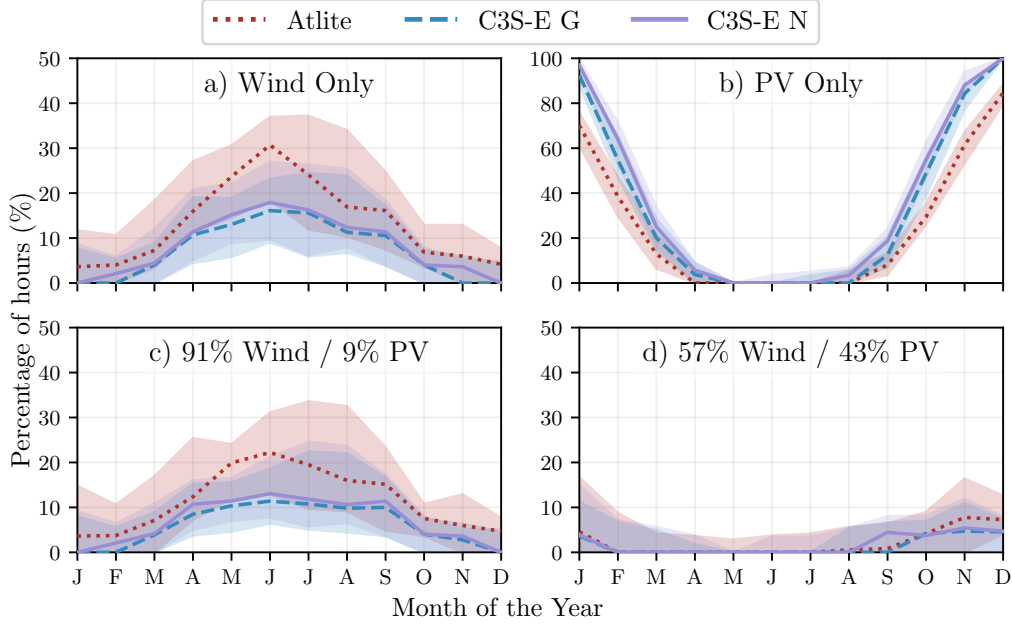


Figure 9: Percentage of hours in a month which are part of a RES drought (from 1979 to 2023) for a) Wind, b) PV, and the combination for the c) 91W-9PV and d) 57W-43PV scenario, for Atlite (red dotted), C3S-E G (blue dashed), and C3S-E N (purple solid). The x-axis represents the month of the year, and the y-axis indicates the percentage of hours. Lines correspond to the median values and the area between the first and third quartiles is shaded.

389 5. Discussion and Conclusions

390 This study has investigated the ability of three RES models to represent
 391 RES droughts: Atlite, C3S-E G, and C3S-E N. One of the most evident dif-
 392 ferences is how each dataset incorporates the specific locations of RES farms.
 393 Both Atlite and C3S-E G consider the locations of wind and PV farms, which
 394 should, in theory, provide a more accurate representation of RES generation.
 395 While this approach slightly improves PV models, our analysis indicates that
 396 for wind energy, the Atlite dataset performs better overall, especially in its
 397 close alignment with observed data for wind generation estimates. This find-
 398 ing suggests that, although the inclusion of RES farm locations is beneficial,
 399 the accuracy of the RES model is more strongly influenced by underlying
 400 model assumptions, such as selecting an appropriate wind power curve.

401 Atlite shows the best alignment with observed data for wind generation.

402 Differences between the models are smaller for PV, with C3S-G performing
403 marginally better than the other two. The results show that the two C3S-
404 E datasets (C3S-E G and C3S-E N) consistently yield similar outcomes,
405 indicating that their methodological differences have minimal impact. This
406 distinction was also evident in the analysis, where Atlite reported higher
407 return periods and a greater number of RES droughts, especially in scenarios
408 with a balanced share of RES. Again, the results from RES drought modelling
409 rely more on the precision of the wind power curve and PV panel models
410 than on the specific locations of RES farms. Atlite’s superior performance
411 highlights the importance of selecting validated models for assessing RES
412 drought risks. This careful model selection can better quantify risks, support
413 effective planning, and avoid the potential underestimation of capacity needs,
414 which is essential for ensuring energy security.

415 Looking at the 57W-43PV scenario, the analysis showed a significant im-
416 provement in the management of RES droughts due to the complementary
417 nature of wind and PV generation. Wind and PV together perform better
418 in terms of reducing drought frequency and duration than either would in-
419 dividually, largely because of the seasonal anti-correlation between the two
420 energy sources. This diversification reduces the seasonal impact on RES
421 droughts, as PV generation peaks in the summer and wind generation is
422 more consistent in winter. Ireland currently has a highly wind-dependent
423 energy system, but with ambitious targets for PV installations in the coming
424 years, the energy mix is expected to approach a balance between wind and
425 PV capacity. While this balanced approach offers a more stable and secure
426 energy supply by mitigating RES drought risks, it is important to note that
427 having similar wind and PV capacities may not optimise other aspects, such
428 as annual energy production or meeting nighttime loads. For policymakers,
429 these findings underscore the importance of meeting these capacity targets
430 to enhance energy security through diversification. Additionally, the choice
431 of model for RES drought assessment becomes increasingly critical as more
432 renewable capacity is integrated into the system.

433 Future work is planned to extend the current analysis. First, climate
434 projection data will be integrated with different energy scenarios, incorpo-
435 rating the addition of offshore wind, to better understand how climate change
436 might affect RES droughts. Second, expanding the geographic domain of the
437 study to include the rest of Europe would provide a more comprehensive un-
438 derstanding of RES droughts in an interconnected energy grid. This would
439 require extensive verification across other European countries, making it a

440 more complex but highly relevant challenge.

441 Data Availability

442 The ERA5 data can be obtained from the Climate Data Store (<https://doi.org/10.24381/cds.adbb2d47>). The C3S-E dataset is also available
443 from the Climate Data Store (<https://doi.org/10.24381/cds.4bd77450>).
444 Information on wind and PV farms in Ireland can be obtained from the
445 EirGrid website ([https://www.eirgrid.ie/grid/system-and-renewable](https://www.eirgrid.ie/grid/system-and-renewable-data-reports)
446 [-data-reports](https://www.eirgrid.ie/grid/system-and-renewable-data-reports)). The Atlite model used in this study is open-source and can
447 be found on GitHub (<https://github.com/pypsa/atlite>). The data and
448 code required to reproduce the analysis in this article will be made available
449 upon acceptance of the manuscript in a public GitHub repository.
450

451 Acknowledgments

452 The research conducted in this publication was funded by Science Foun-
453 dation Ireland and co-funding partners under grant number 21/SPP/3756
454 through the NexSys Strategic Partnership Programme.

455 References

- 456 [1] EuroStat, Renewable Energy Statistics, 2023. URL: [https://ec.europa.eu/eurostat/statistics-explained/index.php?title=Renewable](https://ec.europa.eu/eurostat/statistics-explained/index.php?title=Renewable_energy_statistics)
457 [energy_statistics](https://ec.europa.eu/eurostat/statistics-explained/index.php?title=Renewable_energy_statistics), Accessed: 2024-11-06.
458
- 459 [2] H. C. Bloomfield, D. J. Brayshaw, L. C. Shaffrey, P. J. Coker, H. E.
460 Thornton, Quantifying the increasing sensitivity of power systems to
461 climate variability, *Environmental Research Letters* 11 (2016) 124025.
462 doi:10.1088/1748-9326/11/12/124025.
- 463 [3] H. C. Bloomfield, D. J. Brayshaw, A. Troccoli, C. M. Goodess, M. De Fe-
464 lice, L. Dubus, P. E. Bett, Y.-M. Saint-Drenan, Quantifying the
465 sensitivity of european power systems to energy scenarios and cli-
466 mate change projections, *Renewable Energy* 164 (2021) 1062–1075.
467 doi:10.1016/j.renene.2020.09.125.

- 468 [4] K. van der Wiel, L. P. Stoop, B. R. H. Van Zuijlen, R. Blackport, M. A.
469 Van den Broek, F. M. Selten, Meteorological conditions leading to ex-
470 treme low variable renewable energy production and extreme high en-
471 ergy shortfall, *Renewable and Sustainable Energy Reviews* 111 (2019)
472 261–275. doi:10.1016/j.rser.2019.04.065.
- 473 [5] F. Kaspar, M. Borsche, U. Pfeifroth, J. Trentmann, J. Drücke, P. Becker,
474 A climatological assessment of balancing effects and shortfall risks of
475 photovoltaics and wind energy in germany and europe, *Advances in*
476 *Science and Research* 16 (2019) 119–128. doi:10.5194/asr-16-119-2
477 019.
- 478 [6] M. Ohba, Y. Kanno, D. Nohara, Climatology of dark doldrums in japan,
479 *Renewable and Sustainable Energy Reviews* 155 (2022) 111927. doi:10
480 .1016/j.rser.2021.111927.
- 481 [7] F. Mockert, C. M. Grams, T. Brown, F. Neumann, Meteorological
482 conditions during periods of low wind speed and insolation in Germany:
483 The role of weather regimes, *Meteorological Applications* 30 (2023)
484 e2141. doi:10.1002/met.2141.
- 485 [8] M. J. Mayer, B. Biró, B. Szücs, A. Aszódi, Probabilistic modeling of
486 future electricity systems with high renewable energy penetration using
487 machine learning, *Applied Energy* 336 (2023) 120801. doi:10.1016/j.
488 apenergy.2023.120801.
- 489 [9] D. Raynaud, B. Hingray, B. François, J. Creutin, Energy droughts from
490 variable renewable energy sources in European climates, *Renewable*
491 *Energy* 125 (2018) 578–589. doi:https://doi.org/10.1016/j.renene
492 .2018.02.130.
- 493 [10] K. Z. Rinaldi, J. A. Dowling, T. H. Ruggles, K. Caldeira, N. S. Lewis,
494 Wind and Solar Resource Droughts in California Highlight the Benefits
495 of Long-Term Storage and Integration with the Western Interconnect,
496 *Environmental Science and Technology* 55 (2021) 6214–6226. doi:10.1
497 021/acs.est.0c07848.
- 498 [11] A. Gangopadhyay, A. K. Seshadri, N. J. Sparks, R. Toumi, The role
499 of wind-solar hybrid plants in mitigating renewable energy-droughts,

- Renewable Energy 194 (2022) 926–937. doi:10.1016/j.renene.2022.05.122.
- [12] S. Allen, N. Otero, Standardised indices to monitor energy droughts, Renewable Energy 217 (2023) 119206. doi:10.1016/j.renene.2023.119206.
- [13] J. Kapica, J. Jurasz, F. A. Canales, H. Bloomfield, M. Guezgouz, M. De Felice, Z. Kobus, The potential impact of climate change on european renewable energy droughts, Renewable and Sustainable Energy Reviews 189 (2024) 114011. doi:10.1016/j.rser.2023.114011.
- [14] C. Bracken, N. Voisin, C. D. Burleyson, A. M. Campbell, Z. J. Hou, D. Broman, Standardized benchmark of historical compound wind and solar energy droughts across the Continental United States, Renewable Energy 220 (2024) 119550. doi:<https://doi.org/10.1016/j.renene.2023.119550>.
- [15] H. Hersbach, B. Bell, P. Berrisford, S. Hirahara, A. Horányi, J. Muñoz-Sabater, J. Nicolas, C. Peubey, R. Radu, D. Schepers, et al., The ERA5 global reanalysis, Quarterly Journal of the Royal Meteorological Society 146 (2020) 1999–2049. doi:10.1002/qj.3803.
- [16] L. Dubus, Y. Saint-Drenan, A. Troccoli, M. De Felice, Y. Moreau, L. Ho-Tran, C. Goodess, R. Amaro E Silva, L. Sanger, C3S Energy: A climate service for the provision of power supply and demand indicators for Europe based on the ERA5 reanalysis and ENTSO-E data, Meteorological Applications 30 (2023) e2145. doi:10.1002/met.2145.
- [17] Copernicus Climate Change Service (C3S), Climate and energy indicators for Europe from 1979 to present derived from reanalysis., 2020. doi:10.24381/cds.4bd77450, accessed on 28-11-2024.
- [18] F. Hofmann, J. Hampp, F. Neumann, T. Brown, J. Hörsch, Atlite: a lightweight Python package for calculating renewable power potentials and time series, Journal of Open Source Software 6 (2021) 3294. doi:10.21105/joss.03294.
- [19] J. Li, Z. Zhao, D. Xu, P. Li, Y. Liu, M. A. Mahmud, D. Chen, The potential assessment of pump hydro energy storage to reduce renewable

- 532 curtailment and CO2 emissions in Northwest China, *Renewable Energy*
533 212 (2023) 82–96. doi:10.1016/j.renene.2023.04.132.
- 534 [20] M. Parzen, H. Abdel-Khalek, E. Fedotova, M. Mahmood, M. M. Frysz-
535 tacki, J. Hampp, L. Franken, L. Schumm, F. Neumann, D. Poli,
536 et al., Pypsa-earth. a new global open energy system optimization
537 model demonstrated in africa, *Applied Energy* 341 (2023) 121096.
538 doi:10.1016/j.apenergy.2023.121096.
- 539 [21] K. Ali Khan Niazi, M. Victoria, Comparative analysis of photovoltaic
540 configurations for agrivoltaic systems in europe, *Progress in Photo-*
541 *voltatics: Research and Applications* 31 (2023) 1101–1113. doi:10.1002/
542 pip.3727.
- 543 [22] EirGrid & SONI, System and Renewable Data Reports, 2023. URL:
544 [https://www.eirgrid.ie/grid/system-and-renewable-data-rep](https://www.eirgrid.ie/grid/system-and-renewable-data-reports)
545 [orts](https://www.eirgrid.ie/grid/system-and-renewable-data-reports), Accessed: 2024-11-06.
- 546 [23] P. T. Brown, D. J. Farnham, K. Caldeira, Meteorology and climatology
547 of historical weekly wind and solar power resource droughts over western
548 North America in ERA5, *SN Applied Sciences* 3 (2021) 814. doi:10.1
549 007/s42452-021-04794-z.
- 550 [24] N. Otero, O. Martius, S. Allen, H. Bloomfield, B. Schaeffli, Character-
551 izing renewable energy compound events across Europe using a logistic
552 regression-based approach, *Meteorological Applications* 29 (2022) e2089.
553 doi:10.1002/met.2089, 13.
- 554 [25] Y.-M. Saint-Drenan, L. Wald, T. Ranchin, L. Dubus, A. Troccoli, An
555 approach for the estimation of the aggregated photovoltaic power gener-
556 ated in several European countries from meteorological data, *Advances*
557 *in Science and Research* 15 (2018) 51–62. doi:10.5194/asr-15-51-201
558 8.
- 559 [26] I. Staffell, S. Pfenninger, Using bias-corrected reanalysis to simulate
560 current and future wind power output, *Energy* 114 (2016) 1224–1239.
561 doi:10.1016/j.energy.2016.08.068.
- 562 [27] Gouvernement of Ireland, Climate Action Plan 2024, Technical Report 3,
563 Department of the Environment, Climate and Communications, 2023.

- 564 URL: [https://www.gov.ie/pdf/?file=https://assets.gov.ie/](https://www.gov.ie/pdf/?file=https://assets.gov.ie/284675/70922dc5-1480-4c2e-830e-295afd0b5356.pdf)
565 [284675/70922dc5-1480-4c2e-830e-295afd0b5356.pdf](https://www.gov.ie/pdf/?file=https://assets.gov.ie/284675/70922dc5-1480-4c2e-830e-295afd0b5356.pdf), Accessed:
566 2024-11-06.
- 567 [28] Sustainable Energy Authority Ireland, National Energy Projections
568 2024, Technical Report, Sustainability Energy Authority of Ireland,
569 2024. URL: [https://www.seai.ie/news-and-events/news/energ](https://www.seai.ie/news-and-events/news/energy-projections-report)
570 [y-projections-report](https://www.seai.ie/news-and-events/news/energy-projections-report), Accessed: 2024-11-06.
- 571 [29] H. G. Beyer, G. Heilscher, S. Bofinger, A robust model for the mpp
572 performance of different types of pv-modules applied for the performance
573 check of grid connected systems, Eurosun (2004) 8.